

Inhibitors of the kinase IspE: structure–activity relationships and co-crystal structure analysis†

Anna K. H. Hirsch,^a Magnus S. Alphey,^b Susan Lauw,^c Michael Seet,^a Luzi Barandun,^a Wolfgang Eisenreich,^c Felix Rohdich,^{*c} William N. Hunter,^{*b} Adelbert Bacher^c and François Diederich^{*a}

Received 13th March 2008, Accepted 18th April 2008

First published as an Advance Article on the web 2nd June 2008

DOI: 10.1039/b804375b

Enzymes of the non-mevalonate pathway for isoprenoid biosynthesis are therapeutic targets for the treatment of important infectious diseases. Whereas this pathway is absent in humans, it is used by plants, many eubacteria and apicomplexan protozoa, including major human pathogens such as *Plasmodium falciparum* and *Mycobacterium tuberculosis*. Herein, we report on the design, preparation and biological evaluation of a new series of ligands for IspE protein, a kinase from this pathway. These inhibitors were developed for the inhibition of IspE from *Escherichia coli*, using structure-based design approaches. Structure–activity relationships (SARs) and a co-crystal structure of *Aquifex aeolicus* IspE bound to a representative inhibitor validate the proposed binding mode. The crystal structure shows that the ligand binds in the substrate–rather than the adenosine 5'-triphosphate (ATP)-binding pocket. As predicted, a cyclopropyl substituent occupies a small cavity not used by the substrate. The optimal volume occupancy of this cavity is explored in detail. In the co-crystal structure, a diphosphate anion binds to the Gly-rich loop, which normally accepts the triphosphate moiety of ATP. This structure provides useful insights for future structure-based developments of inhibitors for the parasite enzymes.

Introduction

The development of drugs with a novel mode of action for the treatment of malaria and tuberculosis is of urgent necessity in light of the rapid emergence of multi-drug-resistant parasites.^{1,2} For this purpose, inhibition of the enzymes of the non-mevalonate pathway for the biosynthesis of the essential isoprenoid precursor molecules, isopentenyl diphosphate (IPP) and dimethylallyl diphosphate (DMAPP),³ has been recognised as a highly attractive approach (Scheme 1). This biosynthetic pathway starts with the condensation of pyruvate and glyceraldehyde 3-phosphate and is exclusively used by a number of pathogens, such as the tuberculosis-causing *M. tuberculosis*⁴ and the malaria-causing *P. falciparum*.^{5,6} Both diseases still pose a major health concern as they are responsible for an estimated 300–500 million new infections and 3 million deaths annually.^{1,7} Importantly, the non-mevalonate pathway is completely distinct to that used by humans, making its component enzymes highly attractive drug targets. In fact, the enzymes of the pathway have been validated as drug

targets by Jomaa *et al.*, who showed that fosmidomycin [OHC–N(OH)–(CH₂)₃–PO₃H₂] cures malaria in rodents.⁶ The compound is a potent inhibitor of the second enzyme of the pathway, 1-deoxy-D-xylulose 5-phosphate reductoisomerase (IspC, EC 1.1.1.267), and is currently being tested in clinical trials.⁸ In addition, other series of phosphate and phosphonate-based inhibitors of IspC are under investigation.⁹

The growing number of published X-ray crystal structures of the constituent enzymes of the non-mevalonate pathway¹⁰ has opened up the opportunity for lead generation by structure-based design.¹¹ In recent years, we applied this approach to the development of the first families of ligands for two central enzymes of the pathway, IspE (4-diphosphocytidyl-2C-methyl-D-erythritol kinase, EC 2.7.1.148)^{12,13} and IspF (2C-methyl-D-erythritol 2,4-cyclodiphosphate synthase, EC 4.6.1.12).¹⁴ The kinase IspE requires ATP and Mg²⁺ cations to catalyse the phosphorylation of the 2-OH group of 4-diphosphocytidyl-2C-methyl-D-erythritol (CDP-ME), producing 4-diphosphocytidyl-2C-methyl-D-erythritol-2-phosphate (CDP-ME2P) (Scheme 1).¹⁵

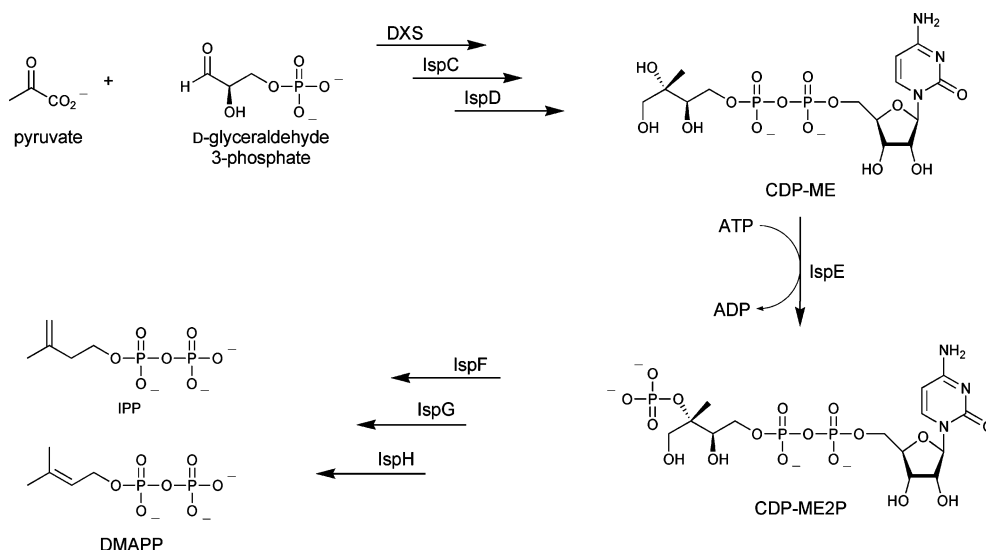
Using the structure-based design approach, we developed first-generation inhibitors of IspE, which target the substrate–rather than the ATP-binding pocket and feature competitive inhibition constants (*K_i*) for the enzyme from *E. coli* down to the upper nanomolar range.¹² To extend this work further, a new series of derivatives was designed to (i) improve their water solubility, (ii) validate the proposed binding mode through SARs and (iii) explore the optimal filling of a small, hydrophobic cavity that is not occupied by the substrate.^{16,17} The synthesis and *in vitro* evaluation of these new inhibitors are reported here. Gratifyingly, enhancement of ligand solubility enabled co-crystallisation with IspE from *A. aeolicus* to give definitive proof of the postulated binding mode.

^aLaboratorium für Organische Chemie, ETH Zürich, HCI, CH-8093, Zürich, Switzerland. E-mail: diederich@org.chem.ethz.ch; Fax: +41 44 6321109

^bDivision of Biological Chemistry and Drug Discovery, College of Life Sciences, MSI/WTB Complex, University of Dundee, Dow Street, Dundee, DD1 5EH, United Kingdom. E-mail: w.n.hunter@dundee.ac.uk; Fax: +44 138 232 2558

^cTechnische Universität München, Lehrstuhl für Organische Chemie und Biochemie, Center for Integrated Protein Research, Lichtenbergstraße 4, D-85748, Garching, Germany. E-mail: felix.rohdich@ch.tum.de; Fax: +49 89 289 1336

† Electronic supplementary information (ESI) available: Synthesis of precursors to the new inhibitors, biological data and evaluation. See DOI: 10.1039/b804375b



Scheme 1 The non-mevalonate pathway for the biosynthesis of the C₅ precursors to isoprenoids, IPP and DMAPP.³ ADP = adenosine 5'-diphosphate, DXS = 1-deoxy-D-xylulose 5-phosphate synthase (EC 2.2.1.7), IspD = 4-diphosphocytidyl-2C-methyl-D-erythritol synthase (EC 2.7.7.60), IspG = 2C-methyl-D-erythritol 2,4-cyclodiphosphate reductase (EC 1.17.4.3), IspH = 1-hydroxy-2-methyl-2-(*E*)-butenyl-4-diphosphate reductase (EC 1.17.1.2).

Results and discussion

Inhibitor design

At the onset of this project, two X-ray crystal structures of IspE were available, one of the apo-enzyme of *Thermus thermophilus* (1.7 Å resolution, RCSB Protein Data Bank (PDB) code: 1UEK)¹⁸ and the other of the ternary complex of *E. coli* IspE bound to CDP-ME and 5'-adenyl-β,γ-amidotriphosphate (AppNp), a non-hydrolysable ATP analogue (2.0 Å resolution, PDB code: 1OJ4, Fig. S1).¹⁹ In the course of this project, two co-crystal structures of *A. aeolicus* IspE and synthetic, cytidine-based ligands were solved (at 2.3 Å and 2.4 Å resolution, PDB codes: 2V2V and

2V2Q, respectively).¹³ The active site of IspE can be divided into three main binding pockets: the adenosine-binding, the cytidine-binding and the ME/phosphate-binding pockets (Fig. S1).

We designed our first-generation inhibitors for *E. coli* IspE, such as (±)-1–(±)-4 (Fig. 1),¹² using the modelling programme MOLOC²⁰ and the crystal structure of the ternary complex mentioned above.¹⁹ They target the cytidine-binding pocket as shown in Fig. 2 for the cyclopropyl derivative (±)-1. This compound was found to be a competitive inhibitor of the kinase with a *K_i* value of 290 ± 100 nM.¹² The central cytosine scaffold was predicted to sandwich between Tyr25 and Phe185 and form three hydrogen bonds to both backbone and side chain of His26, in analogy to

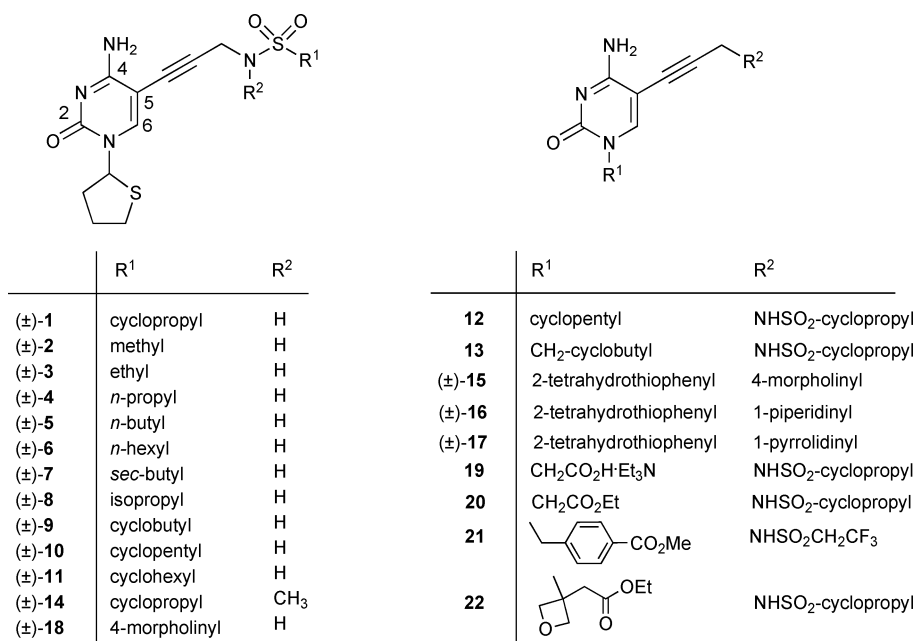


Fig. 1 Inhibitors of IspE investigated in this study.

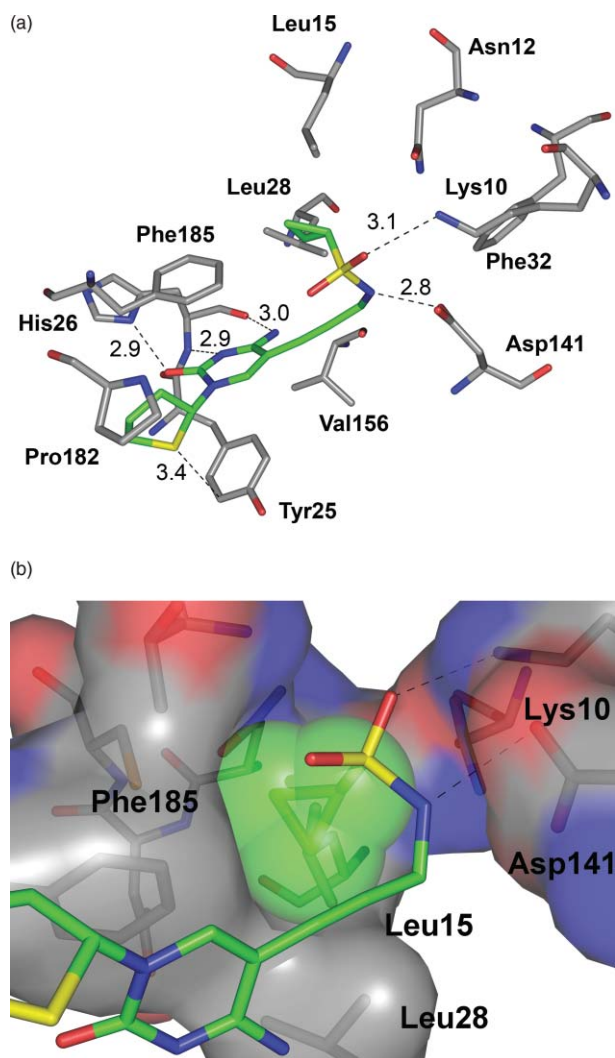


Fig. 2 MOLOC-generated molecular model of inhibitor (\pm)-**112** in the active site of *E. coli* IspE (PDB code: 1OJ4).¹⁹ (a) Overview of the cytidine-binding pocket. (b) Close-up of the small, hydrophobic pocket showing the van der Waals surfaces of the receptor and the cyclopropyl ring of the ligand. Colour code: protein skeleton: C: grey; inhibitor skeleton: C: green; O: red; N: blue; P: orange; S: yellow. Distances are given in Å. The units for the indicated distances and the colour code are maintained throughout the article, if not otherwise stated.

the binding mode observed for the cytosine ring of CDP-ME. A tetrahydrothiophenyl ring was selected as ribose substitute and postulated to occupy the centre of a *pseudo- π* sandwich made of Tyr25 and Pro182. According to the modelling, favourable S–aromatic interactions²¹ with the phenolic ring of Tyr25 are established in both diastereoisomeric complexes formed by (\pm)-**1**, which are expected to be of similar stability. A propargylic sulfonamide vector was chosen to direct an alkyl group, such as the cyclopropyl substituent in (\pm)-**1**, into a newly discovered, small and lipophilic pocket lined by the side chains of Phe185, Leu15 and Leu28. This pocket is not utilised by the substrate CDP-ME. The sulfonamide moiety in its favourable staggered conformation, with the N-lone pair bisecting the O–S–O angle,^{12,22} was expected to form ionic hydrogen bonds to the side chains of Lys10 and Asp141.

Validation and quantification of these postulated individual enzyme–ligand interactions clearly required more extensive SARs and X-ray analysis of co-crystal structures. Thus, compounds (\pm)-**5**–(\pm)-**11** (Fig. 1) were newly prepared to explore the optimal filling of the hydrophobic pocket occupied by the cyclopropyl group of bound (\pm)-**1**. Replacement of the tetrahydrothiophenyl ring in **12** and **13** by alicyclic residues was expected to yield information on the postulated S–aromatic interaction. The N-methylated sulfonamide (\pm)-**14** was designed to evaluate the energetics of the predicted hydrogen bond to the side chain of Asp141. Compounds (\pm)-**15**–(\pm)-**17** lack the sulfonamide group entirely.

IspE is difficult to crystallise and does not even tolerate traces of organic solvents in the crystallisation buffer. This has prevented the analysis of co-crystal structures of the first-generation ligands,¹² even though these compounds are sufficiently soluble in the presence of small amounts of organic co-solvents for conducting *in vitro* assays. Small cytosine derivatives possess remarkably low water-solubility, despite low partition/distribution coefficients (e.g. compound (\pm)-**1**: clogP = clogD = 0.3; Table 1). Therefore, compounds **18**–**22** were specifically prepared with the aim to obtain improved aqueous solubility. Particularly successful in this respect was the introduction of an oxetane derivative as a ribose substitute.²³ The proposed, modelling-supported binding mode of the resulting ligand **22** is depicted in Fig. S2.

Syntheses of the inhibitors

The syntheses of the representative target molecules **22** and (\pm)-**18** are shown in Schemes 2 and 3. The remaining ligands were constructed by an analogous route or following the published synthetic strategy (see the experimental section of the main text for the synthesis and characterisation of the inhibitors, and the ESI for the synthesis and characterisation of the precursors).¹² 5-Iodocytosine (**23**)²⁴ was reacted with the Michael acceptor **24**²³ to afford the alkylated cytosine derivative **25**. The choice of both the right base and temperature turned out to be crucial for this reaction. The alkyne cross-coupling partner **26** was obtained in a reaction of propargyl amine with cyclopropanesulfonyl chloride.¹² The cytosine derivative **25** and the alkyne **26**¹² smoothly underwent Sonogashira cross-coupling, affording inhibitor **22** in good yield (71%, Scheme 2).

For the synthesis of ligand (\pm)-**18**, morpholine was converted into morpholine-4-sulfonyl chloride (**27**) in 84% yield, following a literature procedure.²⁵ This intermediate was reacted with propargyl amine to obtain alkyne **28**. Sonogashira cross-coupling of **28** with cytosine derivative (\pm)-**29**¹² afforded inhibitor (\pm)-**18** in good yield (75%, Scheme 3).

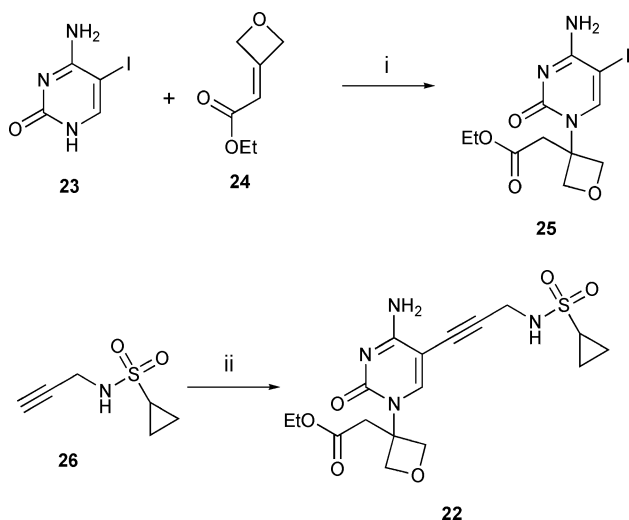
Enzyme assay

The IC₅₀ (IC₅₀ = concentration of inhibitor at which 50% maximum initial velocity is observed) and K_i values for all new inhibitors were determined in a photometric assay, employing a complex set of auxiliary enzymes and *E. coli* IspE (see Table 1 and ESI).²⁶ The inhibition was verified for selected ligands with a direct NMR spectroscopic assay.²⁶ Using the programme Dynafit, the mode of inhibition was assigned (see Fig. S3 and S4 for selected curves to determine IC₅₀ and K_i values).²⁷ While a competitive

Table 1 Inhibitory activities and calculated physicochemical properties of inhibitors for *E. coli* IspE

Ligand	$K_{ic}/\mu\text{M}^a$	$K_{iu}/\mu\text{M}^b$	$\text{IC}_{50}/\mu\text{M}$	Mode ^c	clogP^d	clogD^d
(±)- 1 ¹²	0.29 ± 0.1		8 ± 0	Compet.	0.3	0.3
(±)- 2 ¹²	2.6 ± 0.1		22 ± 2	Compet.	-0.03	-0.06
(±)- 3 ¹²	0.64 ± 0.1		6 ± 0	Compet.	0.5	0.5
(±)- 4 ¹²	8.2 ± 1.7	27.3 ± 11	48 ± 20	Mixed	1.0	1.0
(±)- 5	8.0 ± 0.1		51 ± 1	Compet.	1.6	1.5
(±)- 6	2.0 ± 0.3		47 ± 1	Compet.	2.6	2.6
(±)- 7	1.8 ± 0.3		8 ± 0	Compet.	1.4	1.4
(±)- 8	0.52 ± 0.1		8 ± 0	Compet.	0.9	0.8
(±)- 9	0.56 ± 0		17 ± 1	Compet.	0.9	0.9
(±)- 10	0.89 ± 0.1	19.0 ± 9.2	55 ± 1	Mixed	1.5	1.4
(±)- 11	2.5 ± 0.4	67.7 ± 35	290 ± 1	Mixed	2.0	2.0
12	1.5 ± 0.2		39 ± 0	Compet.	1.0	0.9
13	1.5 ± 0.2		44 ± 6	Compet.	0.9	0.9
(±)- 14	2.5 ± 0.2		13 ± 1	Compet.	1.1	1.1
(±)- 15	41.0 ± 3.0		1300 ± 30	Compet.	0.9	0.9
(±)- 16	4.7 ± 0.3		190 ± 10	Compet.	2.3	2.2
(±)- 17	11.8 ± 0.8		395 ± 20	Compet.	1.7	1.2
(±)- 18	13.1 ± 1.2		110 ± 2	Compet.	-1.0	-1.0
19			597 ± 15		-0.6	-4.0
20			117 ± 3		0.4	0.4
21			144 ± 1		2.3	1.6
22	28.7 ± 1.7		590 ± 10	Compet.	-0.1	-0.2

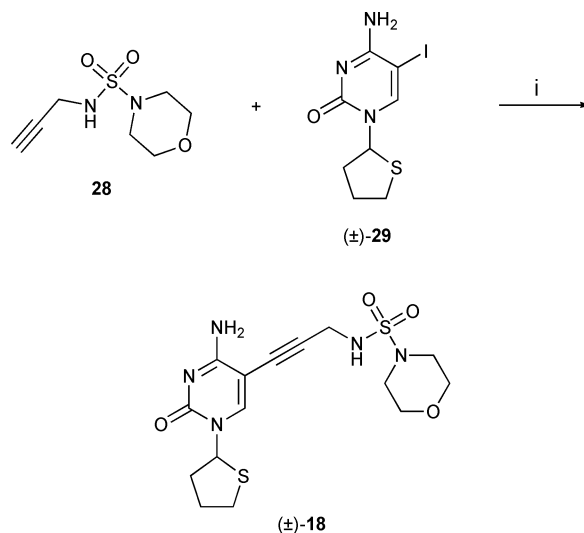
^a K_{ic} = competitive inhibition constant. ^b K_{iu} = uncompetitive inhibition constant. ^c Compet.: competitive inhibition; mixed: mixed competitive–uncompetitive inhibition. ^d The logarithmic partition coefficients clogP (octanol/water) and clogD (octanol/water at pH 7.4) values were calculated with the programmes ACD/LogP and ACD/LogD (ACD-Labs) with an uncertainty of ± 0.7 to 0.9 .



Scheme 2 Synthesis of inhibitor **22**. Reagents and conditions: (i) Cs_2CO_3 , DMF, 25°C , 100 h, 33%; (ii) **25**, Et_3N , $[\text{PdCl}_2(\text{PPh}_3)_2]$, CuI, DMF, 25°C , 16 h, 71%. DMF = *N,N*-dimethylformamide.

mechanism with respect to CDP-ME binding was attributed to most ligands, a mixed competitive (K_{ic})–uncompetitive (K_{iu}) mode of inhibition applied to some exceptions. The kinetics provide a first indication that the ligands occupy the substrate-binding site, as predicted.

The previously described cyclopropyl derivative (±)-**1** remains the best of the inhibitors of *E. coli* IspE reported to date.¹² The three-membered ring seems to provide an optimal filling of the lipophilic pocket lined by the side chains of Phe185, Leu15 and Leu28. The binding affinity of ligands with a smaller alkyl substituent is reduced as the pocket is not properly filled. Thus, the



Scheme 3 Synthesis of inhibitor (±)-**18**. Reagents and conditions: (i) Et_3N , $[\text{Pd}(\text{PPh}_3)_4]$, CuI, DMF, 50°C , 3.5 h, 75%.

K_i value increases by nearly an order of magnitude upon changing from (±)-**1** to methyl-substituted (±)-**2** and by a factor of two upon changing from (±)-**1** to ethyl-substituted (±)-**3** (see Fig. S5 for its proposed binding mode). The affinity of isopropyl- ((±)-**8**) and cyclobutyl- ((±)-**9**) substituted ligands is very similar to that of ethyl-substituted (±)-**3**; in these cases, however, the alkyl residues seem slightly too large for optimal volume occupancy.

Mecozzi and Rebek investigated the ideal volume occupancy of apolar, confined spaces in capsular synthetic receptors. They found that the most stable inclusion complex forms if $55 \pm 9\%$ of the cavity space is occupied by the guest.¹⁶ This so-called “55% rule” holds for numerous complexation events in synthetic

supramolecular chemistry.^{28,29} Recently, it was applied to the filling of a hydrophobic pocket in the active site of an enzyme, the antimalarial target plasmepsin II.¹⁷ At smaller packing coefficients (PCs), the van der Waals interactions in the cavity are less than optimal, while at higher PCs, the mobility of the binding partners becomes reduced, resulting in large entropic losses that counteract enthalpic gains.

By filling the cavity with a hydrocarbon network using the modelling package Spartan 06,^{16,17,30} the free space in the small, lipophilic pocket in *E. coli* IspE was determined to be about 100 Å³. Binding affinity indeed nicely correlates with volume occupancy: the cyclopropyl ring in (±)-**1** shows a PC of 56% and inhibition is most effective ($K_i = 0.29 \mu\text{M}$). Lower PCs (28% for methyl in (±)-**2** and 45% for ethyl in (±)-**3**) or higher PCs (62% for isopropyl in (±)-**8** and 69% for cyclobutyl in (±)-**9**) correlate with weaker inhibition.

When moving to slightly larger sulfonamide substituents, binding affinity decreases strongly. Thus, the K_i values of *n*-propyl-((±)-**4**) and *n*-butyl-((±)-**5**) substituted ligands show a nearly 30-fold increase ($K_i \approx 8 \mu\text{M}$) with respect to (±)-**1**. Modelling suggests that the *n*-propyl residue might still be accommodated in the cavity, although in an energetically less favourable, contorted *gauche* conformation (PC 61%).³¹ Even when folded, the *n*-butyl substituent no longer fits well into the pocket. Hence, a facile conformational change of the propargylic sulfonamide linker could equally well direct this substituent out of the pocket into solvent-exposed space. Larger substituents, such as *n*-hexyl (in (±)-**6**), cyclopentyl (in (±)-**10**) or cyclohexyl (in (±)-**11**), most certainly do not bind in the lipophilic pocket but rather reach into the opposite direction, towards the solvent (see Fig. S6). An increase in binding affinity measured for these ligands largely results from their increased lipophilicity (see the clogP and clogD values in Table 1), and the resulting more favourable partitioning from the aqueous buffer into the less polar protein environment.

The tetrahydrothiophenyl ring remains the best ribose substitute in the investigated family of ligands (for additional ribose replacements, see ref. 12). Similar inhibitory activities are measured for the cyclopentyl- and the cyclobutylmethyl-substituted ligands **12** and **13**. Substitution of the tetrahydrothiophenyl ring in (±)-**1** by a cyclopentyl ring in **12** thus lowers the binding affinity by a factor of five, corresponding to a free enthalpy increment of $\Delta\Delta G_{300\text{K}} \approx 1 \text{ kcal mol}^{-1}$. The two rings are sandwiched between the side chain of Tyr25 and the pyrrolidine ring of Pro182 (see Fig. 2). We explain the increased affinity with favourable interactions between the S atom of the sandwiched heterocyclic ring and the phenolic side chain. The energetics of the proposed S–aromatic interaction are in good agreement with literature values.²¹

Important contributions of the sulfonamide moiety to the observed binding affinity were clearly confirmed. N-methylation in (±)-**14** ($K_i = 2.5 \mu\text{M}$) reduces the inhibitory potency nearly by a factor of ten as compared to (±)-**1**. Therefore, the postulated ionic hydrogen bond between the sulfonamide NH and the side chain of Asp141 (Fig. 2) could contribute as much as $\Delta\Delta G_{300\text{K}} = 1.3 \text{ kcal mol}^{-1}$ to the overall binding free enthalpy. Complete substitution of the sulfonamide moiety for heterocyclic amines in (±)-**15**–(±)-**17** further reduces the inhibitory potency. The piperidine derivative (±)-**16** maintains the largest affinity ($K_i = 4.7 \mu\text{M}$). This finding can be explained with the formation of a favourable ionic hydrogen bond between the protonated piperidinium residue and

the side chain of Asp141 ($d(\text{O}_{\text{Asp}} \cdots \text{N}) = 2.9 \text{ \AA}$ and 3.1 \AA , see Fig. S7).

Finally, efforts to obtain fully water soluble inhibitors for X-ray crystallography were rewarded. Among the five compounds specifically prepared for this purpose, two [(±)-**18** ($K_i = 13.1 \mu\text{M}$) and **22** ($K_i = 28.7 \mu\text{M}$)] did not require addition of Me₂SO to perform the *in vitro* binding assay. Although the former still requires ethanol as a co-solvent, the latter is fully water soluble, enabling X-ray crystallographic studies.

X-Ray crystallography

Building on previous experience,¹³ *A. aeolicus* IspE was chosen to obtain co-crystals with the water-soluble inhibitor **22**. The structure of *A. aeolicus* IspE in complex with **22** was determined to 2.2 Å resolution (PDB code: 2VF3, Fig. S8). The statistics indicate that an acceptable medium resolution model was produced (Table S1). For example, R_{work} and R_{free} values are 22.7 and 27.6%, respectively. The structure is isomorphous with previously determined complexes.¹³ Although adenosine 5'-monophosphate (AMP) was present in the crystallisation conditions, no electron density corresponding to this ligand could be observed.

A. aeolicus IspE displays the typical galactose, homoserine, mevalonate and phosphomevalonate (GHMP) kinase fold that comprises two domains.¹⁹ The N-terminal domain (residues 1–155) consists of an elongated six-stranded β sheet, the concave side of which is flanked by three α helices and two segments of a ₃₁₀ helix. The C-terminal domain comprises an anti-parallel four-stranded β sheet, bordering the N-terminal-domain β sheet, four α helices and two ₃₁₀ helices. The overall distribution of secondary-structure elements is well-conserved in this enzyme family. Although the crystal structure presents two molecules in the asymmetric unit, featuring “active sites A and B”, the enzyme is a monomer as indicated by size exclusion gel chromatography and analytical ultracentrifugation (data not shown). The enzyme active site is a deep, polar cavity located between the N- and C-terminal domains.

The co-crystal structure clearly shows that our proposed binding mode is indeed adopted by the water-soluble inhibitor **22**, *i.e.* it binds at the cytidine-binding pocket (Fig. 3). As discussed previously, the amino acid sequences and structures of the active sites of *A. aeolicus* and *E. coli* IspE show minor differences.¹³ As a result of this, the nucleobase portion and the sulfonamide moiety form slightly different hydrogen-bonding patterns to those predicted by modelling for *E. coli* IspE (see Fig. S2). In particular, the cytosine moiety of **22** is engaged in two additional hydrogen bonds (Fig. 3b). In active site B, the cytosine moiety forms four hydrogen bonds to the side chain and backbone NH and C=O of His25. An additional hydrogen bond is observed between the NH₂ group of the ligand and the backbone C=O of Lys145. The cytosine ring is positioned at the centre of a π sandwich made of Tyr24 and Tyr175 (= Phe185 in *E. coli* IspE). The sulfonamide functionality, at the other end of the inhibitor, is stabilised by hydrogen bonds to the side chains of Asn11, Tyr31 and Asp130 (Fig. 3b).

The sulfonamide moiety of **22** is bound in a similar way in active site A, whereas the nucleobase shows a modified hydrogen-bonding pattern, which could arise from a different conformation of the oxetanyl substituent. As a result, the hydrogen bonds

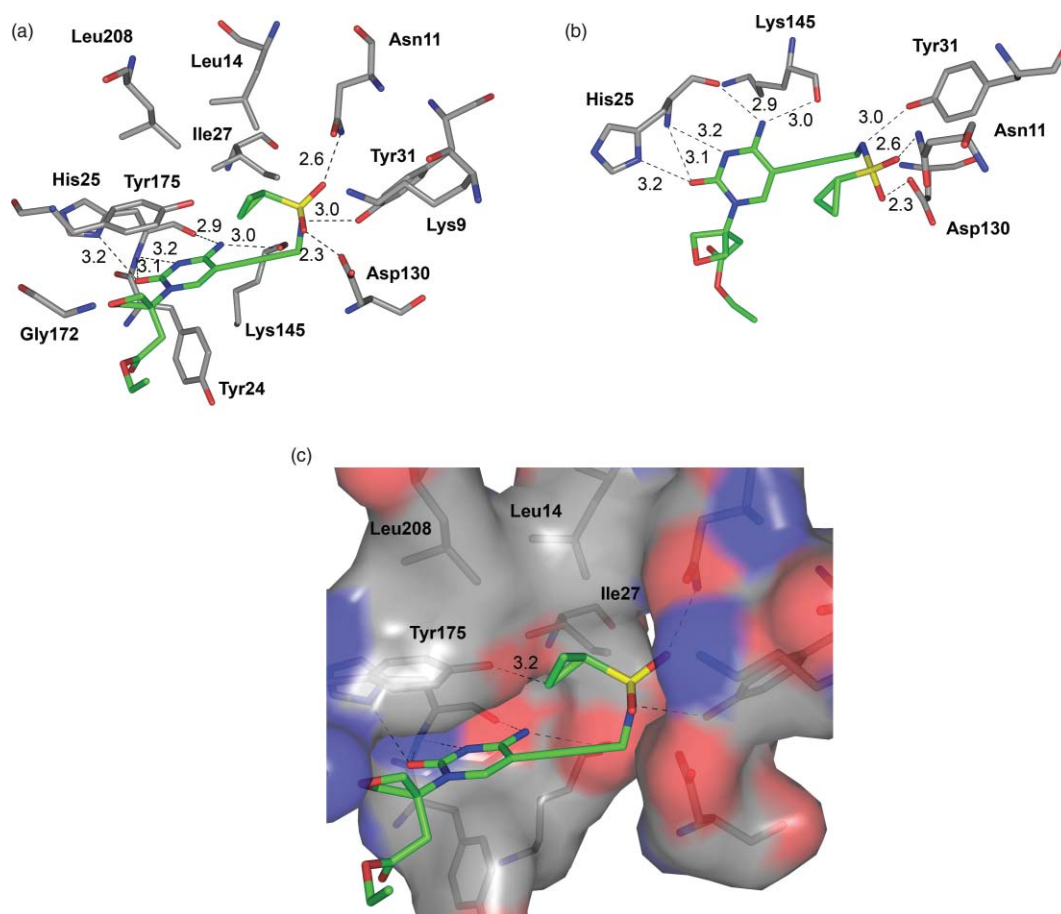


Fig. 3 X-Ray crystal structure of *A. aeolicus* IspE co-crystallised with **22** (PDB code: 2VF3). Shown is active site B (for a view of active site A, see Fig. S8). (a) Overview of the binding mode of **22** in the cytidine-binding pocket. (b) View onto the cytosine and sulfonamide moieties and their hydrogen-bonding interactions with the protein. (c) View onto the cyclopropyl residue approaching the OH group of Tyr175 in the small, lipophilic pocket. The distance between the cyclopropyl substituent and the OH group of Tyr175 is given in Å.

between cytosine and the backbone amide NH of His25 cannot be formed (Fig. S8b). A superposition of **22** in active sites A and B is shown in Fig. S8c. Although the protein backbone is almost perfectly superposed throughout the active sites, some flexibility can be seen at the level of the side chains. Most importantly, the oxetanyl substituent clearly adopts a different conformation to that of **22** bound in active site B.

Electron density was observed in the Gly-rich loop of the adenosine-binding pocket but this was not compatible with AMP that was present in the crystallisation conditions. The density could be modelled, and refined satisfactorily as diphosphate. Indeed, this overlays well with the diphosphate moiety of AppNp in the high-resolution crystal structure of the *E. coli* enzyme complex (data not shown). The diphosphate forms similar hydrogen bonds to the backbone amide NH groups of the Gly-rich loop, a typical motif for the recognition of phosphate groups.³²

A superposition of the co-crystal structure of *A. aeolicus* IspE with **22** and diphosphate (PDB code: 2VF3) and the previously obtained co-crystal structure of a cytidine-based ligand (PDB code: 2V2V)¹³ confirmed our hypothesis that the Gly-rich loop is extremely well conserved and preorganised (Fig. S9a). In addition, it can be observed that the cytidine-binding pocket is equally

well conserved (Fig. S9b). This result consolidates the choice of targeting the inhibitors to the cytidine-binding pocket and establishes *A. aeolicus* IspE as a suitable model system for future rounds of design.

Of particular interest for our future efforts to design inhibitors for IspE from important pathogens such as *M. tuberculosis* or *P. falciparum* is the fact that the cyclopropyl ring of **22** is accommodated in the small, hydrophobic pocket lined by Leu14, Ile27, Tyr175 and Leu208 (Fig. 3c). The residence of the cyclopropyl ring was not necessarily to be expected since the change from Phe185 (in *E. coli* IspE) to Tyr175 (in *A. aeolicus* IspE) makes the pocket much more hydrophilic. Indeed, the cyclopropyl ring prevents any solvation of the phenolic OH group of Tyr175 (Fig. 3c). Because this should be rather unfavourable, it could well explain the reduced inhibitory activity of **22** against *A. aeolicus* IspE. With the propargylic sulfonamide residue, our ligands obviously provide an excellent vector for precisely and favourably addressing this OH group in future studies. This may be important since the enzymes from *M. tuberculosis* and *P. falciparum* possess a conserved tyrosine residue here and according to homology modelling (not shown), the phenolic OH group is directed into the small pocket.

Conclusion

We described the design, synthesis, *in vitro* evaluation and X-ray co-crystal structure analysis of a series of inhibitors of the kinase IspE. These were prepared as a follow-up to the first-generation inhibitors to validate a proposed binding mode. Through interesting SARs, we managed to gain additional evidence for our hypothesis. By designing water-soluble inhibitors and solving the co-crystal structure of one ligand with *A. aeolicus* IspE, the suggested binding mode was validated. The inhibitor occupies the cytidine-binding pocket and exhibits a K_i value in the lower micromolar activity range. This proof of concept opens the way for further modification and optimisation of the inhibitors. The ultimate goal of this research project is the development of ligands with even better activity against IspE from medically important species to make progress on the way to anti-infectives with a novel mode of action.

Experimental

General details

Compounds **1–4**,¹² **23**,²⁴ **24**,²³ **26**,¹² **27**,²⁵ (\pm)-**29**,¹² **30**,³³ **31**,³⁴ **32–33**³⁵ and **34**¹² were prepared according to literature procedures. The synthesis and characterisation of the precursors **35–45** is described in the ESI. Reagents and solvents were purchased reagent grade and used without further purification. THF and CH_2Cl_2 were freshly distilled from sodium benzophenone ketyl and CaH_2 . All reactions were performed in oven-dried glassware under an Ar atmosphere, unless otherwise stated. All products were dried under high vacuum (10^{-2} Torr) before analytical characterisation. TLC: Aluminium sheets coated with SiO_2 -60 UV₂₅₄ from Macherey-Nagel, visualisation by UV light at 245 nm and staining with a solution of KMnO_4 (1.5 g), K_2CO_3 (10 g), 5% NaOH (2.5 cm³) in H_2O (150 cm³) or a solution of ninhydrin (0.3 g) in butanol (100 cm³) and glacial acetic acid (3 cm³). Column chromatography (CC): SiO_2 -60 (230–400 mesh, 0.040–0.063 mm) from Fluka. Uncorrected melting points (mp) were determined in an open capillary using a Büchi-510 apparatus. IR spectra were recorded on a Perkin-Elmer BX FT-IR spectrophotometer (ATR-unit, Attenuated Total Reflection, Golden Gate) as a film or neat. NMR spectra were recorded at 25 °C on a Varian Gemini-300 spectrometer, using the solvent peak as an internal reference. Coupling constants (J) are given in Hz. The resonance multiplicity is described as s (singlet), br s (broad singlet), d (doublet), t (triplet), q (quartet), quint (quintet), sext (sextet) and m (multiplet). High-resolution mass spectra (HR-MS) were recorded on an IonSpec Ultima FT-ICR with 3-hydroxypicolinic acid (3-HPA) as matrix (MALDI), Micromass AutoSpec-Ultima (EI) and Finnigan TSQ 7000 (electrospray ionisation). The detected masses are given as m/z with M^+ representing the molecular ion. Elemental analyses were performed by the Mikrolabor at the Laboratorium für Organische Chemie, ETH Zürich. The nomenclature was generated with the computer programme ACD/Name (ACD/Labs).

Enzyme assays

Materials. [1,3,4-¹³C₃]-CDP-ME was prepared according to a literature procedure.²⁶ *E. coli* IspE was also obtained according

to the published protocol.^{15b} NADH and phosphoenolpyruvate potassium salt were purchased from Biomol, ATP and pyruvate kinase/lactate dehydrogenase from Sigma-Aldrich.

Enzyme-coupled photometric assay for IC₅₀ determination.

Assay mixtures were prepared as described with some modifications:²⁶ 60 mm³ of a solution containing 100 mM Tris-HCl (pH 8.0), 10 mM MgCl_2 , 2 mM dithiothreitol, 2.5 mM phosphoenolpyruvate potassium salt, 2 mM ATP, 0.46 mM NADH, 1 U of lactate dehydrogenase, 1 U of pyruvate kinase and IspE protein were added to 60 mm³ of the inhibitor solutions (final concentration varied from 8–1000 μM). The reaction was started by addition of 60 mm³ of CDP-ME (final concentration 1 mM) and monitored at 340 nm.

Enzyme-coupled photometric assay for K_i determination.

Assay mixtures were prepared as follows: 50 mm³ of a solution containing 100 mM Tris-HCl (pH 8.0), 10 mM MgCl_2 , 2 mM dithiothreitol, 2.5 mM phosphoenolpyruvate potassium salt, 2 mM ATP, 0.46 mM NADH, 1 U of lactate dehydrogenase, 1 U of pyruvate kinase and 2.4 mU IspE protein were added to 50 mm³ each of the inhibitor solution. The reaction was started by addition of 50 mm³ CDP-ME. For the determination of each single K_M value in the presence of the inhibitor, the concentration of CDP-ME was varied from 35–400 μM , while keeping the concentration of the inhibitor fixed. The mixtures were incubated at 27 °C, and the reaction was monitored photometrically at 340 nm. The K_i values of the inhibitors were obtained by observing the behaviour of K_M values at different inhibitor concentrations (0–400 μM) and processing the data using the programme Dynafit.²⁷

¹³C NMR assay. Assay mixtures contained 100 mM Tris-HCl (pH 8.0), 10 mM MgCl_2 , 5 mM ATP, 10% (v/v) D₂O, 2 mM dithiothreitol, 1.5 mM [1,3,4-¹³C₃]-CDP-ME, and 13 μg IspE protein in a volume of 500 mm³. Inhibitory substances were added at final concentrations ranging from 0–3 mM. The mixtures were incubated at 37 °C and terminated by the addition of EDTA to a final concentration of 20 mM. The solution was analysed by ¹³C NMR spectroscopy on a Bruker DRX 500 (125 MHz) spectrometer and referenced to an internal standard of [1-¹³C₁]-glucose (0.9 mM).

General procedures

General procedure A for the Sonogashira cross-coupling of 5-iodocytosine derivatives. To an Ar-degassed Schlenk flask charged with the iodocytosine (1.0 eq.), the acetylene (1.4–2.3 eq.) and Et₃N (3.0–7.0 eq.) in dry DMF, $[\text{PdCl}_2(\text{PPh}_3)_2]$ or $[\text{Pd}(\text{PPh}_3)_4]$ (0.10 eq.) and CuI (0.20 eq.) were added at 25 °C. The mixture was left to stir at 25–50 °C in the dark, the solvent evaporated *in vacuo*, and the residue purified by CC.

If purification by CC yielded the triethylammonium salt, the solid was dissolved in CH_2Cl_2 -*i*-PrOH (3 : 1), washed with saturated aqueous NaCl solution (3 \times), dried over Na_2SO_4 , filtered and concentrated *in vacuo*.

Preparation of the inhibitors

(\pm)-*N*-{3-[4-Amino-2-oxo-1-(tetrahydro-2-thienyl)-1,2-dihydropyrimidin-5-yl]prop-2-yn-1-yl}butane-1-sulfonamide ((\pm)-**5**). General procedure A, starting from (\pm)-**29**¹² (100 mg, 0.30 mmol), **30**³³

(110 mg, 0.60 mmol), Et₃N (0.12 cm³, 0.90 mmol), [PdCl₂(PPh₃)₂] (21 mg, 0.030 mmol) and CuI (11 mg, 0.060 mmol) in dry DMF (8.0 cm³). The mixture was left to stir at 25 °C for 2.5 h. Purification by CC (SiO₂; CH₂Cl₂–MeOH 99 : 1→94 : 6) afforded (±)-**5** (80 mg, 72%) as an off-white solid (Found: C 48.7, H 6.1, N 14.8. Calcd for C₁₅H₂₂N₄O₃S₂: C 48.6, H 6.0, N 15.1%; mp 149–151 °C; $\nu_{\max}(\text{neat})/\text{cm}^{-1}$ 3194, 2959, 2870, 1636, 1496, 1403, 1301, 1228, 1136, 1073, 972, 918, 833, 780, 726, 668; $\delta_{\text{H}}(300 \text{ MHz}, (\text{CD}_3)_2\text{SO})$ 0.84 (t, $J = 7.4$, 3 H), 1.35 (sext, $J = 7.4$, 2 H), 1.60–1.71 (m, 2 H), 1.91–2.07 (m, 3 H), 2.15–2.25 (m, 1 H), 2.81–2.89 (m, 1 H), 3.11 (t, $J = 8.0$, 2 H), 3.18–3.26 (m, 1 H), 4.02 (d, $J = 5.7$, 2 H), 6.13–6.16 (m, 1 H), 6.94 (br s, 1 H), 7.61 (t, $J = 5.7$, 1 H), 7.63 (br s, 1 H), 8.12 (s, 1 H); $\delta_{\text{C}}(75 \text{ MHz}, (\text{CD}_3)_2\text{SO})$ 13.5, 20.9, 25.2, 28.9, 32.7, 32.8, 36.9, 51.1, 64.1, 75.2, 89.1, 91.3, 145.0, 153.5, 163.8; MALDI-HR-MS: calcd for C₁₅H₂₃N₄O₃S₂⁺ ([M + H]⁺): 371.1206; found: 371.1207.

(±)-*N*-{3-[4-Amino-2-oxo-1-(tetrahydro-2-thienyl)-1,2-dihydropyrimidin-5-yl]prop-2-yn-1-yl}hexane-1-sulfonamide ((±)-**6**). General procedure A, starting from (±)-**29**¹² (100 mg, 0.30 mmol), **35** (100 mg, 0.60 mmol), Et₃N (0.12 cm³, 0.90 mmol), [PdCl₂(PPh₃)₂] (21 mg, 0.030 mmol) and CuI (11 mg, 0.060 mmol) in dry DMF (8.0 cm³). The mixture was left to stir at 25 °C for 3 h. Purification by CC (SiO₂; CH₂Cl₂–MeOH 99 : 1→94 : 6) afforded (±)-**6** (49 mg, 41%) as an off-white solid (Found: C 51.4, H 6.5, N 13.8. Calcd for C₁₇H₂₆N₄O₃S₂: C 51.2, H 6.6, N 14.1%; mp 179–182 °C; $\nu_{\max}(\text{neat})/\text{cm}^{-1}$ 3325, 3061, 2929, 2858, 1640, 1496, 1402, 1304, 1228, 1134, 1076, 921, 858, 783; $\delta_{\text{H}}(300 \text{ MHz}, (\text{CD}_3)_2\text{SO})$ 0.78 (t, $J = 6.8$, 3 H), 1.16–1.36 (m, 6 H), 1.61–1.71 (m, 2 H), 1.91–2.06 (m, 3 H), 2.16–2.25 (m, 1 H), 2.82–2.89 (m, 1 H), 3.11 (t, $J = 8.0$, 2 H), 3.19–3.26 (m, 1 H), 4.02 (d, $J = 5.7$, 2 H), 6.13–6.17 (m, 1 H), 6.93 (br s, 1 H), 7.56 (t, $J = 5.7$, 1 H), 7.84 (br s, 1 H), 8.13 (s, 1 H); $\delta_{\text{C}}(75 \text{ MHz}, (\text{CD}_3)_2\text{SO})$ 13.8, 21.9, 23.2, 27.3, 28.9, 30.8, 32.7, 32.8, 36.9, 51.3, 64.1, 75.2, 89.1, 91.3, 145.0, 153.4, 163.8; MALDI-HR-MS: calcd for C₁₇H₂₇N₄O₃S₂⁺ ([M + H]⁺): 399.1519; found: 399.1514.

(±)-*N*-{3-[4-Amino-2-oxo-1-(tetrahydro-2-thienyl)-1,2-dihydropyrimidin-5-yl]prop-2-yn-1-yl}butane-2-sulfonamide ((±)-**7**). General procedure A, starting from (±)-**29**¹² (120 mg, 0.37 mmol), (±)-**36** (94 mg, 0.53 mmol), Et₃N (0.15 cm³, 1.1 mmol), [PdCl₂(PPh₃)₂] (26 mg, 0.037 mmol) and CuI (14 mg, 0.074 mmol) in dry DMF (7.0 cm³). The mixture was left to stir at 25 °C for 2.5 h. Purification by CC (SiO₂; CH₂Cl₂–MeOH 99 : 1→94 : 6) afforded (±)-**7** (99 mg, 72%) as an off-white solid (Found: C 48.7, H 6.1, N 14.8. Calcd for C₁₅H₂₂N₄O₃S₂: C 48.6, H 6.0, N 15.1%; mp 184–186 °C; $\nu_{\max}(\text{neat})/\text{cm}^{-1}$ 3382, 3297, 3207, 3073, 2938, 2861, 1640, 1495, 1405, 1300, 1234, 1122, 1088, 969, 847, 775, 721, 660; $\delta_{\text{H}}(300 \text{ MHz}, (\text{CD}_3)_2\text{SO})$ 0.93 (t, $J = 7.5$, 3 H), 1.24 (d, $J = 6.9$, 3 H), 1.33–1.49 (m, 1 H), 1.88–2.08 (m, 4 H), 2.14–2.25 (m, 1 H), 2.81–2.89 (m, 1 H), 3.03–3.16 (m, 1 H), 3.18–3.26 (m, 1 H), 4.03 (d, $J = 5.4$, 2 H), 6.12–6.16 (m, 1 H), 6.88 (br s, 1 H), 7.57 (t, $J = 5.4$, 1 H), 7.83 (br s, 1 H), 8.11 (s, 1 H); $\delta_{\text{C}}(75 \text{ MHz}, (\text{CD}_3)_2\text{SO})$ 10.9, 12.9, 22.9, 28.9, 32.8 (2 C), 36.9, 57.1, 64.2, 75.1, 89.1, 91.4, 144.9, 153.4, 163.8; MALDI-HR-MS: calcd for C₁₅H₂₃N₄O₃S₂⁺ ([M + H]⁺): 371.1206; found: 371.1206.

(±)-*N*-{3-[4-Amino-2-oxo-1-(tetrahydro-2-thienyl)-1,2-dihydropyrimidin-5-yl]prop-2-yn-1-yl}propane-2-sulfonamide ((±)-**8**). General procedure A, starting from (±)-**29**¹² (97 mg, 0.30 mmol), **37**

(80 mg, 0.50 mmol), Et₃N (0.30 cm³, 2.1 mmol), [PdCl₂(PPh₃)₂] (21 mg, 0.030 mmol) and CuI (11 mg, 0.060 mmol) in dry DMF (8.0 cm³). The mixture was left to stir at 25 °C for 3 h. Purification by CC (SiO₂; CH₂Cl₂–MeOH 99 : 1→94 : 6) afforded (±)-**8** (99 mg, 92%) as an off-white solid; mp 197–200 °C; $\nu_{\max}(\text{neat})/\text{cm}^{-1}$ 3387, 3068, 2974, 1668, 1636, 1506, 1489, 1457, 1439, 1403, 1312, 1232, 1136, 1074, 1057, 973, 889, 778, 692; $\delta_{\text{H}}(300 \text{ MHz}, (\text{CD}_3)_2\text{SO})$ 1.25 (d, $J = 6.9$, 6 H), 1.92–2.07 (m, 3 H), 2.16–2.23 (m, 1 H), 2.81–2.89 (m, 1 H), 3.19–3.32 (m, 2 H), 4.03 (d, $J = 5.7$, 2 H), 6.12–6.16 (m, 1 H), 6.86 (br s, 1 H), 7.55 (t, $J = 5.7$, 1 H), 7.83 (br s, 1 H), 8.11 (s, 1 H); $\delta_{\text{C}}(75 \text{ MHz}, (\text{CD}_3)_2\text{SO})$ 16.2 (2 C), 28.9, 32.8 (2 C), 36.8, 51.5, 64.2, 75.1, 89.1, 91.3, 144.9, 153.5, 163.8; MALDI-HR-MS: calcd for C₁₄H₂₁N₄O₃S₂⁺ ([M + H]⁺): 357.1050; found: 357.1049.

(±)-*N*-{3-[4-Amino-2-oxo-1-(tetrahydro-2-thienyl)-1,2-dihydropyrimidin-5-yl]prop-2-yn-1-yl}cyclobutanesulfonamide ((±)-**9**). General procedure A, starting from (±)-**29**¹² (84 mg, 0.26 mmol), **38** (70 mg, 0.40 mmol), Et₃N (0.11 cm³, 0.80 mmol), [PdCl₂(PPh₃)₂] (19 mg, 0.026 mmol) and CuI (10 mg, 0.050 mmol) in dry DMF (7.0 cm³). The mixture was left to stir at 25 °C for 2.5 h. Purification by CC (SiO₂; CH₂Cl₂–MeOH 99 : 1→94 : 6) afforded (±)-**9** (51 mg, 54%) as an off-white solid (Found: C 48.6, H 5.5, N 14.9. Calcd for C₁₅H₂₀N₄O₃S₂: C 48.9, H 5.5, N 15.2%; mp 184–186 °C; $\nu_{\max}(\text{neat})/\text{cm}^{-1}$ 3382, 3299, 3208, 3066, 2945, 2857, 2707, 1640, 1601, 1504, 1438, 1404, 1343, 1298, 1275, 1227, 1182, 1135, 1081, 1010, 971, 912, 881, 854, 780, 722, 675, 616; $\delta_{\text{H}}(300 \text{ MHz}, (\text{CD}_3)_2\text{SO})$ 1.83–2.09 (m, 5 H), 2.14–2.37 (m, 5 H), 2.81–2.89 (m, 1 H), 3.19–3.27 (m, 1 H), 4.00 (d, $J = 5.7$, 2 H), 4.02 (quint, $J = 8.1$, 1 H), 6.13–6.16 (m, 2 H), 6.88 (br s, 1 H), 7.54 (t, $J = 5.7$, 1 H), 7.83 (br s, 1 H), 8.13 (s, 1 H); $\delta_{\text{C}}(75 \text{ MHz}, (\text{CD}_3)_2\text{SO})$ 16.2, 23.1 (2 C), 28.9, 32.7, 32.8, 36.8, 53.0, 64.2, 75.0, 89.1, 91.5, 145.0, 153.4, 163.7; MALDI-HR-MS: calcd for C₁₅H₂₁N₄O₃S₂⁺ ([M + H]⁺): 369.1050; found: 369.1048.

(±)-*N*-{3-[4-Amino-2-oxo-1-(tetrahydro-2-thienyl)-1,2-dihydropyrimidin-5-yl]prop-2-yn-1-yl}cyclopentanesulfonamide ((±)-**10**). General procedure A, starting from (±)-**29**¹² (84 mg, 0.26 mmol), **39** (73 mg, 0.40 mmol), Et₃N (0.11 cm³, 0.80 mmol), [PdCl₂(PPh₃)₂] (19 mg, 0.026 mmol) and CuI (10 mg, 0.050 mmol) in dry DMF (7.0 cm³). The mixture was left to stir at 25 °C for 2.5 h. Purification by CC (SiO₂; CH₂Cl₂–MeOH 99 : 1→94 : 6) afforded (±)-**10** (75 mg, 75%) as an off-white solid; mp 200–203 °C; $\nu_{\max}(\text{neat})/\text{cm}^{-1}$ 3382, 3290, 3207, 3063, 2948, 2869, 2707, 1640, 1603, 1504, 1472, 1404, 1297, 1250, 1227, 1182, 1121, 1081, 971, 916, 881, 850, 779, 756, 722, 677; $\delta_{\text{H}}(300 \text{ MHz}, (\text{CD}_3)_2\text{SO})$ 1.48–1.73 (m, 4 H), 1.80–2.08 (m, 7 H), 2.14–2.25 (m, 1 H), 2.81–2.89 (m, 1 H), 3.18–3.26 (m, 1 H), 3.68 (quint, $J = 7.7$, 1 H), 4.04 (d, $J = 5.7$, 2 H), 6.12–6.16 (m, 1 H), 6.88 (br s, 1 H), 7.56 (t, $J = 5.7$, 1 H), 7.83 (br s, 1 H), 8.12 (s, 1 H); $\delta_{\text{C}}(75 \text{ MHz}, (\text{CD}_3)_2\text{SO})$ 25.5 (2 C), 27.4 (2 C), 28.9, 32.7 (2 C), 36.9, 60.0, 64.2, 75.1, 89.1, 91.4, 145.0, 153.4, 163.7; MALDI-HR-MS: calcd for C₁₆H₂₃N₄O₃S₂⁺ ([M + H]⁺): 383.1206; found: 383.1198.

(±)-*N*-{3-[4-Amino-2-oxo-1-(tetrahydro-2-thienyl)-1,2-dihydropyrimidin-5-yl]prop-2-yn-1-yl}cyclohexanesulfonamide ((±)-**11**). General procedure A, starting from (±)-**29**¹² (100 mg, 0.30 mmol), **40** (120 mg, 0.60 mmol), Et₃N (0.30 cm³, 2.1 mmol), [PdCl₂(PPh₃)₂] (21 mg, 0.030 mmol) and CuI (11 mg, 0.060 mmol) in dry DMF (8.0 cm³). The mixture was left to stir at 25 °C for 3 h.

Purification by CC (SiO₂; CH₂Cl₂–MeOH 99 : 1 → 94 : 6) afforded (±)-**11** (78 mg, 66%) as an off-white solid; mp 203–205 °C; $\nu_{\text{max}}(\text{neat})/\text{cm}^{-1}$ 3389, 3300, 3212, 3065, 2935, 2854, 2705, 1644, 1605, 1505, 1451, 1403, 1309, 1271, 1248, 1226, 1179, 1136, 1081, 972, 921, 878, 857, 779, 705; $\delta_{\text{H}}(300 \text{ MHz}, (\text{CD}_3)_2\text{SO})$ 1.08–1.40 (m, 5 H), 1.58–1.61 (m, 1 H), 1.75–1.79 (m, 2 H), 1.91–2.23 (m, 6 H), 2.82–2.89 (m, 1 H), 3.04–3.14 (m, 1 H), 3.18–3.25 (m, 1 H), 4.01 (d, $J = 5.7$, 2 H), 6.13–6.17 (m, 1 H), 6.93 (br s, 1 H), 7.56 (t, $J = 5.7$, 1 H), 7.83 (br s, 1 H), 8.13 (s, 1 H); $\delta_{\text{C}}(75 \text{ MHz}, (\text{CD}_3)_2\text{SO})$ 24.5 (2 C), 24.8, 25.9 (2 C), 28.8, 32.8 (2 C), 36.9, 59.1, 64.2, 75.1, 89.1, 91.4, 145.0, 153.5, 163.8; MALDI-HR-MS: calcd for C₁₇H₂₅N₄O₃S⁺ ([M + H]⁺): 397.1363; found: 397.1364.

N-[3-(4-Amino-1-cyclopentyl-2-oxo-1,2-dihydropyrimidin-5-yl)prop-2-yn-1-yl]cyclopropanesulfonamide (12). General procedure A, starting from **41** (100 mg, 0.33 mmol), **26**¹² (100 mg, 0.66 mmol), Et₃N (0.14 cm³, 0.98 mmol), [PdCl₂(PPh₃)₂] (23 mg, 0.033 mmol) and CuI (13 mg, 0.066 mmol) in dry DMF (7.6 cm³). The mixture was left to stir at 25 °C for 2.5 h. Purification by CC (SiO₂; CH₂Cl₂–MeOH 96 : 4) afforded **12** (100 mg, 90%) as an off-white solid (Found C 53.4, H 5.9, N 16.6. Calcd for C₁₅H₂₀N₄O₃S: C 53.6, H 6.0, N 16.7%; mp > 197 °C (decomposition); $\nu_{\text{max}}(\text{neat})/\text{cm}^{-1}$ 3382, 3055, 1669, 1653, 1635, 1617, 1506, 1495, 1456, 1403, 1352, 1238, 1084, 1039, 988, 972, 930, 914, 885, 832, 809, 779, 752, 734, 697, 668, 659; $\delta_{\text{H}}(300 \text{ MHz}, (\text{CD}_3)_2\text{SO})$ 0.94 (d, $J = 6.3$, 4 H), 1.53–1.91 (m, 8 H), 2.63 (quint, $J = 6.3$, 1 H), 4.04 (d, $J = 5.7$, 2 H), 4.72 (quint, $J = 7.8$, 1 H), 6.69 (br s, 1 H), 7.56 (t, $J = 5.7$, 1 H), 7.64 (br s, 1 H), 7.89 (s, 1 H); $\delta_{\text{C}}(75 \text{ MHz}, (\text{CD}_3)_2\text{SO})$ 5.0 (2 C), 23.6 (2 C), 29.5, 30.7 (2 C), 33.0, 57.7, 75.6, 88.8, 91.4, 146.0, 154.1, 164.0; MALDI-HR-MS: calcd for C₁₅H₂₁N₄O₃S⁺ ([M + H]⁺): 337.1329; found: 337.1328.

N-[3-[4-Amino-1-(cyclobutylmethyl)-2-oxo-1,2-dihydropyrimidin-5-yl]prop-2-yn-1-yl]cyclopropanesulfonamide (13). General procedure A, starting from **42** (100 mg, 0.33 mmol), **26**¹² (100 mg, 0.66 mmol), Et₃N (0.14 cm³, 0.98 mmol), [PdCl₂(PPh₃)₂] (23 mg, 0.033 mmol) and CuI (13 mg, 0.066 mmol) in dry DMF (7.6 cm³). The mixture was left to stir at 25 °C for 2.5 h. Purification by CC (SiO₂; CH₂Cl₂–MeOH 96 : 4) afforded **13** (82 mg, 74%) as an off-white solid (Found C 53.8, H 6.0, N 16.7. Calcd for C₁₅H₂₀N₄O₃S: C 53.6, H 6.0, N 16.7%; mp 152–153 °C; $\nu_{\text{max}}(\text{neat})/\text{cm}^{-1}$ 3438, 3056, 2963, 2854, 2323, 1662, 1652, 1622, 1505, 1456, 1444, 1394, 1367, 1326, 1306, 1233, 1192, 1150, 1037, 933, 889, 825, 760, 694, 683, 659; $\delta_{\text{H}}(300 \text{ MHz}, (\text{CD}_3)_2\text{SO})$ 0.95 (d, $J = 6.3$, 4 H), 1.65–1.91 (m, 6 H), 2.58–2.94 (m, 2 H), 3.69 (d, $J = 7.4$, 2 H), 4.03 (d, $J = 5.6$, 2 H), 6.69 (br s, 1 H), 7.57 (t, $J = 5.6$, 1 H), 7.61 (br s, 1 H), 7.97 (s, 1 H); $\delta_{\text{C}}(75 \text{ MHz}, (\text{CD}_3)_2\text{SO})$ 5.0 (2 C), 17.7, 24.8 (2 C), 29.6, 33.0, 34.0, 53.4, 75.4, 88.0, 91.5, 149.1, 154.2, 164.6; MALDI-HR-MS: calcd for C₁₅H₂₁N₄O₃S⁺ ([M + H]⁺): 337.1329; found: 337.1330.

(±)-N-[3-[4-Amino-2-oxo-1-(tetrahydro-2-thienyl)-1,2-dihydropyrimidin-5-yl]prop-2-yn-1-yl]-N-methylcyclopropanesulfonamide ((±)-14). General procedure A, starting from (±)-**29**¹² (120 mg, 0.36 mmol), **43** (87 mg, 0.50 mmol), Et₃N (0.15 cm³, 1.1 mmol), [Pd(PPh₃)₄] (42 mg, 0.036 mmol) and CuI (15 mg, 0.072 mmol) in dry DMF (7.0 cm³). The mixture was left to stir at 50 °C for 26 h. Purification by CC (SiO₂; CH₂Cl₂–MeOH–Et₃N 95 : 5 : 1) afforded (±)-**14** (41 mg, 31%) as an off-white solid; mp 83–85 °C; $\nu_{\text{max}}(\text{neat})/\text{cm}^{-1}$ 3403, 3209, 1644, 1417, 1325, 1272, 1245, 1150,

1106, 1066, 983, 916, 886, 753, 691; $\delta_{\text{H}}(300 \text{ MHz}, \text{CD}_3\text{OD})$ 1.02–1.06 (m, 2 H), 1.08–1.14 (m, 2 H), 1.90–2.15 (m, 3 H), 2.28–2.33 (m, 1 H), 2.58–2.63 (m, 1 H), 2.91–2.96 (m, 1 H), 3.00 (s, 3 H), 3.21–3.27 (m, 1 H), 4.32 (s, 2 H), 6.21–6.24 (m, 1 H), 8.30 (s, 1 H); $\delta_{\text{C}}(75 \text{ MHz}, \text{CD}_3\text{OD})$ 5.5 (2 C), 27.9, 29.8, 34.2, 35.4, 39.2, 41.4, 67.1, 77.4, 90.8, 91.8, 147.2, 156.9, 166.0; MALDI-HR-MS: calcd for C₁₅H₂₁N₄O₃S₂⁺ ([M + H]⁺): 369.1050; found: 369.1050.

(±)-4-Amino-5-(3-morpholin-4-ylprop-1-yn-1-yl)-1-(tetrahydro-2-thienyl)pyrimidin-2(1H)-one ((±)-15). General procedure A, starting from (±)-**29**¹² (68 mg, 0.21 mmol), **31**³⁴ (53 mg, 0.42 mmol), Et₃N (0.90 mm³, 0.63 mmol), [PdCl₂(PPh₃)₂] (15 mg, 0.033 mmol) and CuI (8.0 mg, 0.066 mmol) in dry DMF (4.8 cm³). The mixture was left to stir at 25 °C for 2 h. Purification by CC (SiO₂; CH₂Cl₂–MeOH 95 : 5) afforded (±)-**15** (64 mg, 95%) as an off-white solid; mp 194–196 °C; $\nu_{\text{max}}(\text{neat})/\text{cm}^{-1}$ 3466, 2919, 2853, 2323, 1979, 1656, 1643, 1561, 1555, 1510, 1502, 1477, 1401, 1323, 1300, 1229, 1108, 1072, 1004, 976, 919, 889, 859, 774, 728, 700, 668, 632; $\delta_{\text{H}}(300 \text{ MHz}, \text{CDCl}_3)$ 1.81–1.94 (m, 1 H), 2.02–2.18 (m, 2 H), 2.28–2.40 (m, 1 H), 2.60 (t, $J = 4.4$, 4 H), 2.91–2.99 (m, 1 H), 3.15–3.23 (m, 1 H), 3.49 (s, 2 H), 3.76 (t, $J = 4.4$, 4 H), 5.70 (br s, 1 H), 6.31–6.34 (m, 1 H), 7.56 (br s, 1 H), 8.18 (s, 1 H); $\delta_{\text{C}}(75 \text{ MHz}, (\text{CD}_3)_2\text{SO})$ 29.1, 32.9, 36.7, 47.5, 52.0 (2 C), 64.1, 66.1 (2 C), 76.5, 89.9, 90.8, 145.3, 153.8, 164.1; MALDI-HR-MS: calcd for C₁₅H₂₁N₄O₂S⁺ ([M + H]⁺): 321.1380; found: 321.1384.

(±)-4-Amino-5-(piperidin-1-ylprop-1-yn-1-yl)-1-(tetrahydro-2-thienyl)pyrimidin-2(1H)-one ((±)-16). General procedure A, starting from (±)-**29**¹² (68 mg, 0.21 mmol), **32**³⁵ (52 mg, 0.42 mmol), Et₃N (0.90 mm³, 0.63 mmol), [PdCl₂(PPh₃)₂] (15 mg, 0.021 mmol) and CuI (8.0 mg, 0.042 mmol) in dry DMF (4.8 cm³). The mixture was left to stir at 25 °C for 2 h. Purification by CC (SiO₂; CH₂Cl₂–MeOH 91 : 9) afforded (±)-**16** (29 mg, 43%) as a brown oil; $\nu_{\text{max}}(\text{thin film})/\text{cm}^{-1}$ 3441, 3288, 3081, 2934, 2854, 1653, 1634, 1558, 1539, 1521, 1505, 1496, 1399, 1363, 1308, 1263, 1229, 1149, 1125, 1036, 993, 939, 889, 803, 780, 732, 697, 653; $\delta_{\text{H}}(300 \text{ MHz}, \text{CDCl}_3)$ 1.45–1.47 (m, 2 H), 1.63–1.69 (m, 4 H), 1.80–1.93 (m, 1 H), 2.00–2.18 (m, 2 H), 2.30–2.42 (m, 1 H), 2.55 (m, 4 H), 2.91–2.99 (m, 1 H), 3.15–3.22 (m, 1 H), 3.47 (s, 2 H), 5.86 (br s, 1 H), 6.31–6.34 (m, 1 H), 7.28 (br s, 1 H), 8.16 (s, 1 H); $\delta_{\text{C}}(75 \text{ MHz}, \text{CDCl}_3)$ 23.7, 25.7 (2 C), 28.3, 33.4, 38.9, 48.5, 53.7, 66.0 (2 C), 75.7, 90.9, 91.6, 145.3, 155.1, 164.4; MALDI-HR-MS: calcd for C₁₆H₂₃N₄OS⁺ ([M + H]⁺): 319.1587; found: 319.1586.

(±)-4-Amino-5-(pyrrolidin-1-ylprop-1-yn-1-yl)-1-(tetrahydro-2-thienyl)pyrimidin-2(1H)-one ((±)-17). General procedure A, starting from (±)-**29**¹² (68 mg, 0.21 mmol), **33**³⁵ (46 mg, 0.42 mmol), Et₃N (0.90 mm³, 0.63 mmol), [PdCl₂(PPh₃)₂] (15 mg, 0.021 mmol) and CuI (8.0 mg, 0.042 mmol) in dry DMF (4.8 cm³). The mixture was left to stir at 25 °C for 2 h. Purification by CC (SiO₂; CH₂Cl₂–MeOH 91 : 9) afforded (±)-**17** (34 mg, 53%) as a brown oil; $\nu_{\text{max}}(\text{thin film})/\text{cm}^{-1}$ 3289, 3143, 1662, 1646, 1653, 1635, 1506, 1457, 1404, 1363, 1317, 1229, 1127, 1034, 1008, 903, 804, 783, 668, 649; $\delta_{\text{H}}(300 \text{ MHz}, \text{CDCl}_3)$ 1.83–2.03 (m, 5 H), 2.04–2.16 (m, 2 H), 2.28–2.38 (m, 1 H), 2.66 (m, 4 H), 2.91–2.99 (m, 1 H), 3.15–3.23 (m, 1 H), 3.61 (s, 2 H), 5.76 (br s, 1 H), 6.31–6.35 (m, 1 H), 7.16 (br s, 1 H), 8.16 (s, 1 H); $\delta_{\text{C}}(75 \text{ MHz}, (\text{CD}_3)_2\text{SO})$ 23.1 (2 C), 28.9, 32.7, 36.6, 43.2, 52.1 (2 C), 64.0, 76.3, 89.5, 90.2, 145.3, 153.6, 163.9; MALDI-HR-MS: calcd for C₁₅H₂₁N₄OS⁺ ([M + H]⁺): 305.1431; found: 305.1432.

(\pm)-*N*-{3-[4-Amino-2-oxo-1-(tetrahydro-2-thienyl)-1,2-dihydropyrimidin-5-yl]prop-2-yn-1-yl}morpholine-4-sulfonamide ((\pm)-**18**). General procedure A, starting from (\pm)-**29**¹² (120 mg, 0.37 mmol), **28** (110 mg, 0.54 mmol), Et₃N (0.15 cm³, 1.1 mmol), [Pd(PPh₃)₄] (43 mg, 0.037 mmol) and CuI (14 mg, 0.054 mmol) in dry DMF (7.0 cm³). The mixture was left to stir at 50 °C for 3.5 h. Purification by CC (SiO₂; CH₂Cl₂–MeOH 92 : 8) afforded (\pm)-**18** (110 mg, 75%) as an off-white solid; mp 197–199 °C; ν_{max} (neat)/cm^{−1} 3327, 2846, 2551, 2401, 2149, 1639, 1489, 1402, 1348, 1322, 1261, 1229, 1175, 1137, 1111, 1068, 1023, 993, 924, 837, 779, 728, 688, 627; δ_{H} (300 MHz, (CD₃)₂SO) 1.92–2.05 (m, 3 H), 2.15–2.22 (m, 1 H), 2.80–2.88 (m, 1 H), 3.06 (t, *J* = 4.5, 4 H), 3.18–3.22 (m, 1 H), 3.30 (s, 1 H), 3.62 (t, *J* = 4.5, 4 H), 3.98 (d, *J* = 3.6, 2 H), 6.12–6.15 (m, 1 H), 6.83 (br s, 1 H), 7.84 (t, *J* = 3.6, 1 H), 8.12 (s, 1 H); δ_{C} (75 MHz, (CD₃)₂SO) 28.9, 32.8, 33.2, 37.0, 45.7 (2 C), 64.4, 65.5 (2 C), 75.3, 89.3, 91.7, 145.2, 153.8, 164.0; MALDI-HR-MS: calcd for C₁₅H₂₂N₅O₄S⁺ ([M + H]⁺): 400.1108; found: 400.1113.

Triethylammonium [4-amino-5-{3-[(cyclopropylsulfonyl)amino]prop-1-yn-1-yl}-2-oxo-1,2-dihydropyrimidin-1(2*H*)-yl]acetate (**19**). A solution of **20** (70 mg, 0.20 mmol) in aq. Et₃N solution (1 M, 9.0 cm³) was heated to reflux for 1 h. The resulting mixture was concentrated *in vacuo*, co-evaporated with ethanol (3 × 10 cm³) and dried to afford **19** (60 mg, 90%) as a white solid; mp > 220 °C (decomposition); ν_{max} (neat)/cm^{−1} 3286, 3202, 3060, 2449, 1728, 1660, 1609, 1495, 1427, 1393, 1309, 1241, 1187, 1142, 1050, 949, 892, 834, 799, 784, 760, 716, 624; δ_{H} (300 MHz, (CD₃)₂SO) 0.95 (d, *J* = 5.7, 4 H), 2.59–2.63 (m, 1 H), 4.04 (d, *J* = 5.7, 2 H), 4.35 (s, 2 H), 6.81 (br s, 1 H), 7.59 (t, *J* = 5.7, 1 H), 7.73 (br s, 1 H), 7.92 (s, 1 H); δ_{C} (75 MHz, (CD₃)₂SO) 5.1 (2C), 29.6, 33.0, 50.1, 75.1, 88.5, 91.6, 149.8, 154.2, 165.0, 169.8; MALDI-HR-MS: calcd for C₁₂H₁₅N₄O₅S⁺ ([M + H]⁺): 327.0758; found: 327.0763.

Ethyl [4-amino-5-{3-[(cyclopropylsulfonyl)amino]prop-1-yn-1-yl}-2-oxo-1,2-dihydropyrimidin-1(2*H*)-yl]acetate (**20**). General procedure A, starting from **44** (323 mg, 1.0 mmol), **26**¹² (318 mg, 2.0 mmol), Et₃N (0.42 cm³, 3.0 mmol), [Pd(PPh₃)₄] (120 mg, 0.10 mmol) and CuI (38 mg, 0.20 mmol) in dry DMF (20 cm³). The mixture was left to stir at 50 °C for 3.5 h. Purification by CC (SiO₂; CH₂Cl₂–MeOH 90 : 10) afforded **20** (267 mg, 75%) as a white solid; mp 221–223 °C; ν_{max} (neat)/cm^{−1} 3421, 3053, 2875, 2233, 1750, 1668, 1644, 1508, 1489, 1440, 1422, 1397, 1382, 1356, 1327, 1308, 1205, 1166, 1144, 1061, 1035, 936, 888, 838, 785, 739, 701, 675; δ_{H} (300 MHz, (CD₃)₂SO) 0.95 (d, *J* = 6.3, 4 H), 1.18 (t, *J* = 7.1, 3 H), 2.62 (quint, *J* = 6.3, 1 H), 4.04 (s, 2 H), 4.11 (q, *J* = 7.1, 2 H), 4.46 (s, 2 H), 6.88 (br s, 1 H), 7.58 (br s, 1 H), 7.80 (br s, 1 H), 7.96 (s, 1 H); δ_{C} (75 MHz, (CD₃)₂SO) 5.1 (2 C), 14.1, 29.6, 32.9, 49.9, 61.0, 74.8, 88.7, 91.7, 149.3, 153.8, 164.8, 168.1; MALDI-HR-MS: calcd for C₁₄H₁₉N₄O₅S⁺ ([M + H]⁺): 355.1071; found: 355.1067.

Methyl 4-{[4-amino-2-oxo-5-(3-[(2,2,2-trifluoroethyl)sulfonyl]amino]prop-1-yn-1-yl]pyrimidin-1(2*H*)-yl]methyl}benzoate (**21**). General procedure A, starting from **45** (310 mg, 0.81 mmol), 2,2,2-trifluoro-*N*-prop-2-yn-1-ylethanesulfonamide (**34**)¹² (260 mg, 1.3 mmol), Et₃N (0.34 cm³, 2.5 mmol), [PdCl₂(PPh₃)₂] (58 mg, 0.081 mmol) and CuI (32 mg, 0.16 mmol) in dry DMF (17 cm³). The mixture was left to stir at 25 °C for 20 h. Purification by CC (SiO₂; CH₂Cl₂–MeOH 90 : 10) afforded **21** (270 mg, 73%) as an

off-white solid; mp 198–200 °C; ν_{max} (neat)/cm^{−1} 3403, 3301, 3006, 2563, 1725, 1639, 1603, 1506, 1437, 1389, 1355, 1338, 1318, 1273, 1245, 1198, 1186, 1152, 1132, 1108, 1067, 1020, 986, 934, 889, 846, 799, 781, 752, 690, 668; δ_{H} (300 MHz, (CD₃)₂SO) 3.83 (s, 3 H), 4.10 (d, *J* = 5.1, 2 H), 4.49 (q, *J* = 9.9, 2 H), 4.95 (s, 2 H), 6.86 (br s, 1 H), 7.38 (d, *J* = 8.1, 2 H), 7.78 (br s, 1 H), 7.92 (d, *J* = 8.1, 2 H), 8.19 (s, 1 H), 8.33 (t, *J* = 5.1, 1 H); δ_{C} (75 MHz, (CD₃)₂SO) 32.6, 51.4, 52.0, 52.8 (q, *J* = 30.3), 75.3, 88.7, 90.6, 122.2 (q, *J* = 276.4), 127.5 (2 C), 128.5, 129.2 (2 C), 142.7, 149.3, 153.9, 164.6, 165.8; MALDI-HR-MS: calcd for C₁₈H₁₈F₃N₄O₅S⁺ ([M + H]⁺): 459.0945; found: 459.0947.

Ethyl [3-[4-amino-5-{3-[(cyclopropylsulfonyl)amino]prop-1-yn-1-yl}-2-oxopyrimidin-1(2*H*)-yl]oxetan-3-yl]acetate (**22**). General procedure A, starting from **25** (46 mg, 0.12 mmol), **26**¹² (44 mg, 0.28 mmol), Et₃N (50 mm³, 0.36 mmol), [PdCl₂(PPh₃)₂] (7.0 mg, 0.01 mmol) and CuI (4 mg, 0.02 mmol) in dry DMF (3 cm³). The mixture was left to stir at 25 °C for 16 h. Purification by CC (SiO₂; CH₂Cl₂–MeOH 95 : 5) afforded **22** (35 mg, 71%) as an off-white solid; mp 146–148 °C; ν_{max} (neat)/cm^{−1} 3103, 2930, 2388, 2284, 1712, 1645, 1542, 1495, 1410, 1372, 1326, 1302, 1245, 1203, 1148, 1086, 1069, 1021, 980, 906, 887, 836, 785, 732, 708; δ_{H} (300 MHz, CDCl₃) 0.98–1.04 (m, 2 H), 1.17–1.26 (m, 5 H), 2.51–2.60 (m, 1 H), 3.40 (s, 2 H), 4.08 (q, *J* = 7.2, 2 H), 4.12 (d, *J* = 4.2, 2 H), 4.62 (d, *J* = 7.5, 2 H), 4.88 (d, *J* = 7.5, 2 H), 6.54 (br s, 1 H), 6.68 (br s, 1 H), 6.99 (br s, 1 H), 7.56 (s, 1 H); δ_{C} (75 MHz, CDCl₃) 5.2 (2 C), 13.7, 30.0, 32.9 (2 C), 38.5, 60.6, 60.9, 74.1, 78.4 (2 C), 91.8, 146.2, 153.4, 164.5, 170.1; MALDI-HR-MS: calcd for C₁₇H₂₃N₄O₆S⁺ ([M + H]⁺): 411.1338; found: 411.1333.

Ethyl [3-(4-amino-5-iodo-2-oxopyrimidin-1(2*H*)-yl)oxetan-3-yl]acetate (**25**). A suspension of **23**²⁴ (190 mg, 0.80 mmol) and Cs₂CO₃ (144 mg, 0.44 mmol) in dry DMF (9.0 cm³) was left to stir at 25 °C for 1 h. Compound **24**²³ (0.042 cm³, 0.40 mmol) in dry DMF (2.0 cm³) was added, and the mixture was left to stir at 25 °C for 100 h. The resulting mixture was concentrated *in vacuo*. Purification by CC (SiO₂; CH₂Cl₂–MeOH 95 : 5) afforded **25** (50 mg, 33%) as a yellow solid (Found C 35.2, H 4.05, N 10.8. Calcd for C₁₁H₁₄IN₃O₄: C 34.9, H 3.75, N 11.1%; mp > 175 °C (decomposition); ν_{max} (neat)/cm^{−1} 3403, 3212, 1712, 1644, 1418, 1353, 1318, 1272, 1244, 1151, 1132, 1151, 1105, 1083, 1066, 982, 917, 886, 863, 752, 691, 614; δ_{H} (300 MHz, CD₃OD) 1.21 (t, *J* = 7.1, 3 H), 3.34 (s, 2 H), 4.12 (q, *J* = 7.1, 2 H), 4.60 (d, *J* = 7.8, 2 H), 4.92 (d, *J* = 7.8, 2 H), 7.81 (s, 1 H); δ_{C} (75 MHz, (CD₃)₂SO) 14.0, 56.0, 60.2, 60.4, 62.7, 77.7 (2 C), 148.9, 153.1, 164.0, 169.5; MALDI-HR-MS: calcd for C₁₁H₁₅IN₃O₄⁺ ([M + H]⁺): 380.0102; found: 380.0098.

N-Prop-2-yn-1-ylmorpholine-4-sulfonamide (**28**). To a solution of propargyl amine (0.10 cm³, 1.5 mmol) and Et₃N (0.23 cm³, 1.7 mmol) in dry CH₂Cl₂ (10 cm³), **27**²⁵ (280 mg, 1.5 mmol) was slowly added at 0 °C. The mixture was left to stir at 40 °C for 18 h and concentrated *in vacuo*. The residue was taken up in CH₂Cl₂ (50 cm³) and washed with saturated aqueous NaCl solution (3 × 30 cm³). The organic phase was dried over Na₂SO₄, filtered and concentrated *in vacuo* and afforded **28** (140 mg, 46%) as a yellow solid; mp 70–72 °C; ν_{max} (neat)/cm^{−1} 3276, 3257, 2963, 2929, 2857, 1622, 1458, 1430, 1314, 1304, 1261, 1213, 1140, 1125, 1110, 1088, 1075, 1018, 995, 936, 924, 840, 722, 711, 659, 628; δ_{H} (300 MHz, CDCl₃) 2.35 (t, *J* = 2.4, 1 H), 3.25 (t, *J* = 4.2, 4 H), 3.76 (t, *J* = 4.2,

4 H), 3.87 (dd, $J = 2.4, 6.3, 2$ H), 4.71 (br s, 1 H); δ_c (75 MHz, CDCl_3) 33.0, 45.9 (2 C), 66.0 (2 C), 72.7, 79.4; electrospray-ionisation-HR-MS: calcd for $\text{C}_7\text{H}_{13}\text{N}_2\text{O}_3\text{S}^+$ ($[\text{M} + \text{H}]^+$): 205.0641; found: 205.0658.

X-Ray crystal structure of the complex with 22

Sample preparation. A plasmid encoding *A. aeolicus* IspE with an N-terminal histidine tag with a protease cleavage site was used to produce recombinant enzyme. Purification by affinity and ion exchange chromatography gave a yield of 15 mg dm^{-3} of enzyme.³⁶

Crystallisation, data collection and processing. *A. aeolicus* IspE at 30 mg dm^{-3} in 10 mM Tris-HCl , 20 mM NaCl , $1 \text{ mM dithiothreitol}$, pH 8.5, was incubated with AMP and 22 each at 4 mM for 1 h on ice, filtered using a $0.1 \mu\text{m}$ spin filter (Millipore) then crystallised using hanging drop vapour diffusion at 18°C . Crystals grew in 2 days in 2 mm^3 drops consisting of 1 mm^3 protein complex and 1 mm^3 reservoir solution ($1.6 \text{ M } (\text{NH}_4)_2\text{SO}_4$, $0.1 \text{ M Na cacodylate}$, pH 6.5, 0.1 M NaBr). The pyramidal crystals typically grew to dimensions of $0.4 \times 0.4 \times 0.4 \text{ mm}$. Crystals were cryo-protected in artificial mother liquor containing 20% glycerol and flash cooled for data collection on beam-line BM14 at the European Synchrotron Radiation Facility, Grenoble, using a MAR CCD 225 detector. Data to 2.2 \AA were processed and scaled using *MOSFLM*³⁷ and *SCALA*,³⁸ respectively (Table S1). The crystals are cubic in space group $P2_13$ with two molecules in the asymmetric unit and a unit cell length $a = 137.3 \text{ \AA}$ and are isomorphous with the previously solved *A. aeolicus* IspE structure (to be published elsewhere).

Structure determination. The CCP4 suite of programmes was used for the analysis.³⁹ Rigid body and rounds of restrained refinement,⁴⁰ interspersed with model building in *COOT*,⁴¹ allowed two molecules of 22, nine halide ions and 156 water molecules to be included in the model. The head group of 22 was well-defined in the electron density and given full occupancy, but parts of the tail appeared to be more flexible and occupancy of 0.75 was assigned to this region of the inhibitor. AMP was in the crystallisation conditions but there was no electron density corresponding to adenine. A diphosphate and water molecules could be modelled in the ATP binding site. The use of NaCl and NaBr in the crystallisation conditions resulted in six Cl^- and three Br^- ions being assigned. The complex was refined to an R_{factor} and R_{free} of 22.7% and 27.6%, respectively. Model geometry was assessed using *PROCHECK*,⁴² and all residues were found in the most favourable or allowed regions of the Ramachandran plot. Crystallographic statistics are presented in Table S1, and coordinates and structure factors have been deposited in the PDB under accession code 2VF3.

Acknowledgements

This work was supported by the following agencies: ETH Research council (to A.K.H.H. and F.D.), F. Hoffmann-La Roche Ltd, Basel, Hans-Fischer Gesellschaft (to S.L., A.B., F.R. and W.E.), The Wellcome Trust (to M.S.A and W.N.H.), Biotechnology and Biological Sciences Research Council (UK) (to M.S.A and W.N.H.) and the European Synchrotron Radiation Facility. We

thank Prof. Erick M. Carreira and Georg Wuitschik, ETH Zürich, for kindly providing compound 24.

References

- (a) U. Weiss, *Nature*, 2002, **415**, 669; (b) J. K. Baird, *New Engl. J. Med.*, 2005, **352**, 1565–1577; (c) <http://www.cdc.gov/malaria/impact/index.htm>; (d) M. Schlitzer, *ChemMedChem*, 2007, **2**, 944–986.
- (a) A. L. Kritski, L. S. Rodrigues de Jesus, M. K. Andrade, E. Werneck-Barroso, M. A. Vieira, A. Haffner and L. W. Riley, *Chest*, 1997, **111**, 1162–1167; (b) J. E. Ollé-Goig, *Trop. Med. Int. Health*, 2006, **11**, 1625–1628.
- (a) M. Rohmer, M. Knani, P. Simonin, B. Sutter and H. Sahm, *Biochem. J.*, 1993, **295**, 517–524; (b) M. K. Schwarz, ETH Zurich, Ph.D. dissertation, No. 10951, 1994; (c) S. T. J. Broers, PhD dissertation, No. 10978, ETH Zurich, 1994; (d) W. Eisenreich, B. Menhard, P. J. Hylands, M. H. Zenk and A. Bacher, *Proc. Natl. Acad. Sci. U. S. A.*, 1996, **93**, 6431–6436; (e) W. Eisenreich, M. Schwarz, A. Cartayrade, D. Arigoni, M. H. Zenk and A. Bacher, *Chem. Biol.*, 1998, **5**, R221–R233.
- Y. Boucher and W. F. Doolittle, *Mol. Microbiol.*, 2000, **37**, 703–716.
- (a) F. Rohdich, J. Wungsintaweeikul, M. Fellermeier, S. Sagner, S. Herz, K. Kis, W. Eisenreich, A. Bacher and M. H. Zenk, *Proc. Natl. Acad. Sci. U. S. A.*, 1999, **96**, 11758–11763; (b) F. Rohdich, S. Hecht, A. Bacher and W. Eisenreich, *Pure Appl. Chem.*, 2003, **75**, 393–405.
- H. Jomaa, J. Wiesner, S. Sanderbrand, B. Altincicek, C. Weidemeyer, M. Hintz, I. Türbachova, M. Eberl, J. Zeidler, H. K. Lichtenthaler, D. Soldati and E. Beck, *Science*, 1999, **285**, 1573–1576.
- http://www.cdc.gov/tb/WorldTBDay/resources_global.htm.
- (a) For some selected publications on fosmidomycin and derivatives: T. Kuzuyama, T. Shimizu, S. Takahashi and H. Seto, *Tetrahedron Lett.*, 1998, **39**, 7913–7916; (b) M. A. Missinou, S. Borrmann, A. Schindler, S. Issifou, A. A. Adegnika, P.-B. Matsiegui, R. Binder, B. Lell, J. Wiesner, T. Baranek, J. Jomaa and P. G. Kremsner, *Lancet*, 2002, **360**, 1941–1942; (c) J. Wiesner, R. Ortmann, H. Jomaa and M. Schlitzer, *Angew. Chem., Int. Ed.*, 2003, **42**, 5274–5293; (d) B. Lell, R. Ruangwearayut, J. Wiesner, M. A. Missinou, A. Schindler, T. Baranek, M. Hintz, D. Hutchinson, H. Jomaa and P. G. Kremsner, *Antimicrob. Agents Chemother.*, 2003, **47**, 735–738; (e) S. Oyakhirrome, S. Issifou, P. Pongratz, F. Barondi, M. Ramharter, J. F. Kun, M. A. Missinou, B. Lell and P. G. Kremsner, *Antimicrob. Agents Chemother.*, 2007, **51**, 1869–1871; (f) N. Singh, G. Cheve, M. A. Avery and C. R. McCurdy, *Curr. Pharm. Des.*, 2007, **13**, 1161–1177.
- (a) Y.-H. Woo, R. P. M. Fernandes and P. J. Proteau, *Bioorg. Med. Chem.*, 2006, **14**, 2375–2385; (b) V. Devreux, J. Wiesner, J. L. Goeman, J. Van der Eycken, H. Jomaa and S. Van Calenbergh, *J. Med. Chem.*, 2006, **49**, 2656–2660; (c) T. Haemers, J. Wiesner, S. Van Poecke, J. Goeman, D. Henschker, E. Beck, H. Jomaa and S. Van Calenbergh, *Bioorg. Med. Chem. Lett.*, 2006, **16**, 1888–1891.
- W. N. Hunter, *J. Biol. Chem.*, 2007, **282**, 21573–21577.
- F. Hof and F. Diederich, *Chem. Commun.*, 2004, 477–480.
- A. K. H. Hirsch, S. Lauw, P. Gersbach, W. B. Schweizer, F. Rohdich, W. Eisenreich, A. Bacher and F. Diederich, *ChemMedChem*, 2007, **2**, 806–810.
- C. M. Crane, A. K. H. Hirsch, M. S. Alphey, T. Sgraja, S. Lauw, V. Illarionova, F. Rohdich, W. Eisenreich, W. N. Hunter, A. Bacher and F. Diederich, *ChemMedChem*, 2008, **3**, 91–101.
- (a) C. M. Crane, J. Kaiser, N. L. Ramsden, S. Lauw, F. Rohdich, W. Eisenreich, W. N. Hunter, A. Bacher and F. Diederich, *Angew. Chem., Int. Ed.*, 2006, **45**, 1069–1074; (b) C. Baumgartner, C. Eberle, F. Diederich, S. Lauw, F. Rohdich, W. Eisenreich and A. Bacher, *Helv. Chim. Acta*, 2007, **90**, 1043–1068.
- (a) F. Rohdich, J. Wungsintaweeikul, H. Lüttgen, M. Fischer, W. Eisenreich, C. A. Schuhr, M. Fellermeier, N. Schramek, M. H. Zenk and A. Bacher, *Proc. Natl. Acad. Sci. U. S. A.*, 2000, **97**, 8251–8256; (b) H. Lüttgen, F. Rohdich, S. Herz, J. Wungsintaweeikul, S. Hecht, C. A. Schuhr, M. Fellermeier, S. Sagner, M. H. Zenk, A. Bacher and W. Eisenreich, *Proc. Natl. Acad. Sci. U. S. A.*, 2000, **97**, 1062–1067; (c) T. Kuzuyama, M. Takagi, K. Kaneda, H. Watanabe, T. Dairi and H. Seto, *Tetrahedron Lett.*, 2000, **41**, 2925–2928.
- S. Mecozzi and J. Rebek Jr., *Chem.–Eur. J.*, 1998, **4**, 1016–1022.
- M. Zürcher, T. Gottschalk, S. Meyer, D. Bur and F. Diederich, *ChemMedChem*, 2008, **3**, 237–240.

- 18 T. Wada, T. Kuzuyama, S. Satoh, S. Kuramitsu, S. Yokoyama, S. Unzai, J. R. H. Tame and S.-Y. Park, *J. Biol. Chem.*, 2003, **278**, 30022–30027.
- 19 L. Miallau, M. S. Alphey, L. E. Kemp, G. A. Leonard, S. M. McSweeney, S. Hecht, A. Bacher, W. Eisenreich, F. Rohdich and W. N. Hunter, *Proc. Natl. Acad. Sci. U. S. A.*, 2003, **100**, 9173–9178.
- 20 (a) P. R. Gerber and K. Müller, *J. Comput. Aided Mol. Des.*, 1995, **9**, 251–268; (b) Gerber Molecular Design (<http://www.moloc.ch>).
- 21 E. A. Meyer, R. K. Castellano and F. Diederich, *Angew. Chem., Int. Ed.*, 2003, **42**, 1210–1250.
- 22 V. Petrov, V. Petrova, G. V. Girichev, H. Oberhammer, N. I. Giricheva and S. Ivanov, *J. Org. Chem.*, 2006, **71**, 2952–2956.
- 23 G. Wuitschik, M. Rogers-Evans, K. Müller, H. Fischer, B. Wagner, F. Schuler, L. Polonchuk and E. Carreira, *Angew. Chem., Int. Ed.*, 2006, **45**, 7736–7739.
- 24 K. A. Watanabe, T.-L. Su, R. S. Klein, C. K. Chu, A. Matsuda, M. W. Chun, C. Lopez and J. J. Fox, *J. Med. Chem.*, 1983, **26**, 152–156.
- 25 J. U. Jeong, *Int. Pat.*, WO 2005/013909, 2005.
- 26 V. Illarionova, J. Kaiser, E. Ostrozhenkova, A. Bacher, M. Fischer, W. Eisenreich and F. Rohdich, *J. Org. Chem.*, 2006, **71**, 8824–8834.
- 27 P. Kuzmic, *Anal. Biochem.*, 1996, **237**, 260–273.
- 28 (a) O. Hayashida, L. Sebo and J. Rebek Jr., *J. Org. Chem.*, 2002, **67**, 8291–8298; (b) A. Scarso, L. Trembleau and J. Rebek Jr., *Angew. Chem., Int. Ed.*, 2003, **42**, 5499–5502; (c) L. Trembleau and J. Rebek Jr., *Science*, 2003, **301**, 1219–1220; (d) A. Scarso, L. Trembleau and J. Rebek Jr., *J. Am. Chem. Soc.*, 2004, **126**, 13512–13518; (e) B. W. Purse and J. Rebek Jr., *Proc. Natl. Acad. Sci. U. S. A.*, 2006, **103**, 2530–2534; (f) R. J. Hooley and J. Rebek Jr., *Org. Lett.*, 2007, **9**, 1179–1182.
- 29 (a) L. Pirondini, D. Bonifazi, B. Cantadori, P. Braiuca, M. Campagnolo, R. De Zorzi, S. Geremia, F. Diederich and E. Dalcanele, *Tetrahedron*, 2006, **62**, 2008–2015; (b) T. Gottschalk, B. Jaun and F. Diederich, *Angew. Chem., Int. Ed.*, 2007, **46**, 260–264.
- 30 *Spartan '06*, Wavefunction Inc., Irvine, CA, USA, 2006.
- 31 For the binding of linear alkanes in confined spaces, see: J. Rebek Jr., *Chem. Commun.*, 2007, 2777–2789.
- 32 A. K. H. Hirsch, F. R. Fischer and F. Diederich, *Angew. Chem., Int. Ed.*, 2007, **46**, 338–352.
- 33 J. Deng, J. Tabei, M. Shiotsuki, F. Sanda and T. Masuda, *Macromolecules*, 2004, **37**, 5538–5543.
- 34 P. Malherbe and R. Masciadri, *Int. Pat.*, WO2005/094828, 2005.
- 35 (a) A. Viola, J. J. Collins, N. Filipp and J. S. Locke, *J. Org. Chem.*, 1993, **58**, 5067–5075; (b) J. H. Biel and F. DiPierro, *J. Am. Chem. Soc.*, 1958, **80**, 4609–4614.
- 36 T. Sgraja, M. S. Alphey, S. Ghilagaber, R. Marquez, M. N. Robertson, J. L. Hemmings, S. Lauw, F. Rohdich, A. Bacher, W. Eisenreich, V. Illarionova and W. N. Hunter, *FEBS J.*, 2008, **275**, 2779–2794.
- 37 A. G. W. Leslie, *Joint CCP4 and ESF-EAMCB Newsletter on Protein Crystallography*, 1992, **No. 26**.
- 38 P. Evans, *Acta Crystallogr., Sect. D: Biol. Crystallogr.*, 2006, **62**, 72–82.
- 39 Collaborative Computational Project, Number 4: *Acta Crystallogr., Sect. D: Biol. Crystallogr.*, 1994, **50**, 760–763.
- 40 G. N. Murshudov, A. A. Vagin and E. J. Dodson, *Acta Crystallogr., Sect. D: Biol. Crystallogr.*, 1997, **53**, 240–255.
- 41 P. Emsley and K. Cowtan, *Acta Crystallogr., Sect. D: Biol. Crystallogr.*, 2004, **60**, 2126–2132.
- 42 R. A. Laskowski, D. S. Moss and J. M. Thornton, *J. Mol. Biol.*, 1993, **231**, 1049–1067.